ADVANCES IN ATMOSPHERIC SCIENCES, VOL. 34, MAY 2017, 623–634

• **Original Paper** •

GPS Water Vapor and Its Comparison with Radiosonde and ERA-Interim Data in Algeria

Houaria NAMAOUI*[1,2], Salem KAHLOUCHE[2], Ahmed Hafid BELBACHIR[1], Roeland Van MALDEREN[3], Hugues BRENOT[4], and Eric POTTIAUX[5]

[1]*Faculté de Physique, Université des Sciences et de la Technologie d'Oran Mohamed Boudiaf, USTO-MB, BP 1505, El M'naouer,* 31000 *Oran, Algérie*

[2]*Département de Géodésie Spatiale, Centre des Techniques Spatiales,* 31200 *Arzew, Algérie*

[3]*Royal Meteorological Institute of Belgium,* 1180*, Uccle, Belgium*

[4]*Royal Belgian Institute for Space Aeronomy,* 1180*, Uccle, Belgium*

[5]*Royal Observatory of Belgium,* 1180*, Uccle, Belgium*

(Received 26 April 2016; revised 17 November 2016; accepted 24 November 2016)

ABSTRACT

Remote sensing of atmospheric water vapor using global positioning system (GPS) data has become an effective tool in meteorology, weather forecasting and climate research. This paper presents the estimation of precipitable water (PW) from GPS observations and meteorological data in Algeria, over three stations located at Algiers, Bechar and Tamanrasset. The objective of this study is to analyze the sensitivity of the GPS PW estimates for the three sites to the weighted mean temperature (T_m), obtained separately from two types of T_m–T_s regression [one general, and one developed specifically for Algeria (T_s stands for surface temperature)], and calculated directly from ERA-Interim data. The results show that the differences in T_m are of the order of 18 K, producing differences of 2.01 mm in the final evaluation of PW. A good agreement is found between GPS-PW and PW calculated from radiosondes, with a small mean difference with Vaisala radiosondes. A comparison between GPS and ERA-Interim shows a large difference (4 mm) in the highlands region. This difference is possibly due to the topography. These first results are encouraging, in particular for meteorological applications in this region, with good hope to extend our dataset analysis to a more complete, nationwide coverage over Algeria.

Key words: GPS, atmospheric water vapor, radiosonde, ERA-Interim

Citation: Namaoui, H., S. Kahlouche, A. H. Belbachir, R. Van Malderen, H. Brenot, and E. Pottiaux, 2017: GPS water vapor and its comparison with radiosonde and ERA-Interim data in Algeria. *Adv. Atmos. Sci.*, **34**(5), 623–634, doi: 10.1007/s00376-016-6111-1.

1. Introduction

Water vapor plays an important role in atmospheric processes, but its quantification is difficult because of its temporal variation in space and time, depending on the complex interaction of several phenomena like convection, precipitation and turbulence. Radiosonde profiles, as classical methods of collecting data on atmospheric water vapor, do not generally offer the spatial and temporal resolution necessary for in-depth studies of weather and climate (Ware et al., 2000). These sondes are launched twice a day at most sites, and are located hundreds of miles from each other. Moreover, these methods are affected by issues of calibration, poor quality of data, and long-term reliability (Elliott, 1995, Wang and Zhang, 2008).

In recent years, the use of the global positioning system (GPS) satellites to sense water vapor in the troposphere has increased. In addition to its use for geodetic positioning, it also allows the estimation of atmospheric water vapor. Specifically, it is possible to convert the propagation delay of electromagnetic waves in atmospheric precipitable water (PW) when at least the surface temperature [T_s, from which the weighted mean temperature (T_m) can be derived] and pressure at the same site are known (Bevis et al., 1992; Rocken et al., 1997). Many studies have shown that GPS is an efficient tool that can complement other remote sensing techniques for measuring the water vapor content, which is a useful quantity for climatological and weather forecasting applications (Guerova et al., 2003, 2016). Recent experiments have proved the ability of GPS to measure the water vapor with the same accuracy as other instruments, such

* Corresponding author: Houaria NAMAOUI
Email: houaria.namaoui@univ-usto.dz, hnamaoui@cts.asal.dz

© Institute of Atmospheric Physics/Chinese Academy of Sciences, and Science Press and Springer-Verlag Berlin Heidelberg 2017

as radiosondes, radiometers and photometers (Torres et al., 2010; Van Malderen et al., 2014).

The first objective of this study is to provide preliminary retrievals of PW from GPS receivers in Algeria using different estimations of T_m. Specifically, T_m is determined by linear regression from T_s using the known equation model of Bevis et al. (1992), and using the equation model established for Algeria by Boutiouta and Lahcene (2013). T_m is also calculated directly by numerical integration of the vertical profiles of temperature and humidity, measured by radiosondes or taken from the numerical weather model output of ERA-Interim. The second objective of this study is then the validation of those different parameterizations by comparing the resulting GPS-PW retrievals with the PW values obtained with radiosonde data and from ERA-Interim data.

2. Methodology

2.1. *Physics of the atmospheric propagation delay*

The troposphere is the lower part of the neutral atmosphere, extending from Earth's surface up to an altitude of approximately 16 km at the equator and 8 km at the poles, and composed of dry gases and water vapor (Kos et al., 2009).

Global Navigation Satellite System (GNSS) signals are affected by refraction due to molecules in the troposphere, and this introduces delay in the arrival time of the signal due to bending and delay along the propagation path. The path is determined from knowledge of the refraction index (n), which is conveniently expressed in terms of refractivity (N) (Bevis et al., 1994):

$$N = 10^6(n-1)\,. \tag{1}$$

An often used expression for N has the following form (Thayer, 1974):

$$N(z) = 10^6(n-1) = k_1\frac{P_d(z)}{T} + k_2\frac{P_w(z)}{T} + k_3\frac{P_w(z)}{T^2}\,, \tag{2}$$

where P_d, T and P_w are the partial pressure of dry air, temperature, and the partial pressure of water vapor, respectively, and vary with height z. The coefficients $k_1 = (77.60 \pm 0.05)\mathrm{K\ hPa^{-1}}$, $k_2 = (64.8 \pm 0.08)\mathrm{K\ Pa^{-1}}$ and $k_3 = (373900 \pm 0.04)\mathrm{K^2\ Pa^{-1}}$.

2.2. *Zenith total delay (ZTD)*

The phase delay along the zenith direction is related to the atmospheric refractivity, $N(z)$, by

$$\mathrm{ZTD} = 10^{-6}\int_{\text{receiver}}^{\infty} N(z)dz\,. \tag{3}$$

The refractivity can be divided into two parts—the hydrostatic (N_{hydr}) and the wet delay (N_{wet}):

$$N = N_{hydr} + N_{wet}. \tag{4}$$

The zenith hydrostatic delay (ZHD) is the delay due to the whole density of the neutral atmosphere and can be accurately estimated, under the assumption of hydrostatic equilibrium, from only the surface pressure P_{sur} and the variation of the gravity field f with respect to the latitude φ and the height above the geoid h (in km), (Saastamoinen, 1972; Davis et al., 1985):

$$\mathrm{ZHD} = (0.0022768 \pm 0.0000024)\frac{P_{sur}}{f(\varphi,h)}\,, \tag{5}$$

$$f(\varphi,h) = 1 - 0.00266\cos\varphi - 0.00026h\,. \tag{6}$$

The zenith wet delay (ZWD) represents the contribution of water vapor, and is expressed by

$$\mathrm{ZWD} = 10^{-6}\left[k_2\int\left(\frac{P_w}{T}\right)dz + k_3\int\left(\frac{P_w}{T^2}\right)dz\right], \tag{7}$$

where P_w and T are the partial pressure of water vapor (in hPa) and the atmospheric temperature (in K), respectively. k_2 and k_3 are the coefficients of refractivity obtained experimentally; their errors are negligible in the error budget for processing of the PW (Bevis et al., 1994; Brenot et al., 2006):

$$\begin{aligned} k_2 &= (64.8 \pm 0.08)\,,\\ k_3 &= (373900 \pm 0.04)\,. \end{aligned} \tag{8}$$

3. Determination of PW from ZWD

The total PW (generally expressed in mm) is the amount of liquid water that would be obtained if all the water vapor in the atmosphere within a vertical column were compressed to the point of condensation. Considering the density of water being equal to 1 g $\mathrm{cm^{-3}}$, PW is equivalent to the integrated water vapor (IWV) content (generally expressed in kg $\mathrm{m^{-2}}$). The relationship between PW and the wet delay can be expressed as follows (Askne and Nordius, 1987):

$$\mathrm{PW} = k\mathrm{ZWD}\,, \tag{9}$$

$$k = [10^6(k_3/T_m + k_2')R_v\rho]^{-1}\,, \tag{10}$$

where R_v (= 461.5181 kg $\mathrm{K^{-1}}$) is the gas constant for the water vapor, ρ is air density, $k_2' = (17 \pm 10)$ and T_m is the weighted mean temperature of the atmosphere. The weighted mean temperature T_m is defined as (Davis et al., 1985)

$$T_m = \frac{\int\frac{P_V}{T}dz}{\int\frac{P_V}{T^2}dz}\,, \tag{11}$$

where p_v is the partial pressure of water vapor, T is the absolute temperature, and z is the vertical coordinate. T_m can either be calculated from vertical profile data provided by radiosondes or global reanalysis data, or estimated from T_s (in K) observations using a linear empirical relationship (e.g. Bevis et al., 1992)—the so-called T_m–T_s relationship:

$$T_m = 70.2 + 0.72T_s\,. \tag{12}$$

This Bevis et al. (1992) regression was based on an analysis of 8718 radiosonde profiles spanning approximately a two-year interval from 13 sites in the United States with a latitudinal range of 27° (West Palm Beach, Florida) to 65°

(Fairbanks, Alaska) and a height range of these stations from 0 to 1.6 km.

Based on a period of three years (2005–07) of radiosonde observations at five permanent sites in Algeria (Dar-El-Beida, Bechar, Tindouf, In-Salah and Tamanrasset), Boutiouta and Lahcene (2013) derived the following T_m–T_s relationship for Algeria:

$$T_m = 14.79 + 0.96T_s \, . \tag{13}$$

4. Dataset and instruments

4.1. *GPS and radiosonde data*

We use the GPS data from three stations in Algeria: Algiers, Bechar and Tamanrasset. These data, from the National Institute of Cartography and Remote Sensing and the Algerian Research Centre for Astronomy, Astrophysics and Geophysics, are obtained using LEICA GRX1200+GNSS and ASHTECH UZ-12 receivers.

The observations of Tamanrasset station are available from 21 November to 4 December 2012, while for Algiers and Bechar the available data period is the entire month of August for the same year. The climatic characteristics for 2012 for these stations can be summarized as follows:

(1) For Algiers, the average maximum temperature is 37°C and the accumulated precipitation for the year is 666 mm. The PW variability is high at this station throughout the year, with a daily amplitude of around 30 mm between the very humid month of August and that of December (value based on radiosonde observations).

(2) For Bechar, located in the torrid (subtropical) zone, the average maximum temperature is around 47°C, and the station is sometimes affected by the ramifications of the monsoon in West Africa. The accumulated precipitation is about 144 mm for 2012. Unfortunately, the radiosonde observations for the year 2012 for this station contain some errors, so we are unable to draw conclusions for the PW variability for this year.

(3) The climate around Tamanrasset station is very dry throughout the year, but tempered with altitude. The mean temperature is about 28°C and the annual accumulated precipitation amounts to 42 mm. The annual variation of PW at Tamanrasset is similar to Algiers, with a maximal difference of 28 mm between summer and winter (value based on radiosonde observations for the year 2012).

It can therefore be concluded that these three stations are located in distinct regions from a climatological point of view.

To process the GPS data, we include the three stations of VILL (Villafranca, Spain), RABT (Rabat, Morocco) and CAGL (Cagliari, Italy) from the International GNSS Service (IGS). Additional details regarding the processing of the GPS data using Bernese software, version 5, can be found in Table 1.

The three Algerian GPS stations used have the advantage that they are co-located with radiosonde sites within 10 km. Information on the GPS–radiosonde site distances and height differences is summarized in Table 2. The radiosonde data are from the University of Wyoming, which hosts a website showing the latest radiosonde observations (http://weather.uwyo.edu/upperair/sounding.html). Because of the (small) height difference between the GPS and co-located meteorological site, an altitude correction of the surface values obtained at the meteorological site should be made. The T_s correction is made by assuming a constant temperature lapse rate with altitude for a humid atmosphere (-6.5 K km^{-1}). This is the most appropriate value for the three Algerian stations used here, as we calculate from the radiosonde profiles lapse rates of -6.15, -6.67 and -7.01 K km^{-1} for Algiers, Bechar and Tamanrasset, respectively.

The correction of the surface pressure, measured at the meteorological station, to the GPS antenna height, is based

Table 1. GPS processing parameters.

	GPS processing parameters
Software	Bernese GPS software, version 5.0
Processing method	Network solution
Satellite and receiver antenna phase center calibration	IGS08 absolute phase center offset and variation model
Tropospheric model	The troposphere delay have been modeled by a model of Saastamoinen (1972) with Niell mapping functions (1996).
Tropospheric gradient	Horizontal gradient parameters tilting (2-h interval)
Mapping functions	Wet–Niell mapping functions (1-h interval)
Elevation cut-off angle	10°

Table 2. Location of GPS and radiosonde sites used in this study. The latitudes and longitudes are given in decimal degrees; the height is given with respect to the WGS84 ellipsoid. For the radiosonde sites, the distance (Dist.) and altitude difference (Diff. alt.) are given with the co-located GPS sites.

GPS sites				Radiosondes sites		
Station	Latitude (°E)	Longitude (°N)	Height (m)	WMO code	Dist. (km)	Diff. alt. (m)
Algiers	36.7	3.10	71.90	60390	9.75	42.9
Bechar	31.6	−2.24	863.45	60571	7.15	47.45
Tamanrasset	22.7	5.2	1415.99	60680	1.1	37.99

on the hypsometric equation (Vey et al., 2009):

$$P_{\mathrm{GPS}} = \frac{P e^{-g\Delta H}}{R_{\mathrm{d}} T} , \qquad (14)$$

where P_{GPS} is the pressure at the GPS antenna height (hPa), R_{d} (= 287.058 J kg^{-1} K^{-1}) is the gas constant for dry air, P is the pressure at the height of the pressure sensor (hPa), $\Delta H = H_{\mathrm{GPS}} - H_{\mathrm{s}}$ is the height difference (in m), and T is the actual mean temperature of the layer between the GPS antenna and the meteorological sensor (in K).

Because all of the radiosonde sites are located at a higher altitude than the co-located GPS site (by about 40 m), the PW values obtained at the radiosonde site are expected to be smaller than those retrieved at the co-located GPS site, possibly leading to a bias offset between the PW values at both sites. From the radiosondes profiles, we calculate biases/offsets that could be expected for a height difference less than 50 m between the GPS site and the radiosonde launch site. We find mean offsets of the order of 0.38, 0.20 and 0.10 mm for Algiers, Bechar and Tamanrasset, respectively. These offset differences are due to the more humid atmosphere at Algiers and the low variation in PW at the other two sites.

4.2. *ERA-Interim*

We use ERA-Interim data to retrieve the IWV time series at the three Algerian GPS sites and to calculate the T_{m} values at those sites. ERA-Interim is a global atmospheric reanalysis from 1979 to present, produced by a numerical weather prediction model run at the European Centre for Medium-Range Weather Forecasts (Dee et al., 2011). The horizontal resolution of ERA-Interim is $0.75° \times 0.75°$, with a temporal resolution of 6 h. The PW values are interpolated from the four grid points surrounding the GPS station (see Fig. 1), weighted with the inverse distance to the GPS station, and corrected for the altitude difference between the surface grids and the GPS station. For the calculation of the T_{m}, the integration starts at the height of the GPS station, or the meteorological parameters are extrapolated from the surface grid height to the GPS station height.

5. Comparison of the different T_{m} calculations

In this section, we use different models of T_{m} [which we name Bevis, Boutiouta and ERA-Interim for the Bevis et al. (1992) regression, the Boutiouta and Lahcene (2013) regression, and the ERA-Interim calculation, respectively]. Figure 2 shows the time series of the different T_{m} estimations. First, it can be noted that the T_{m} calculated by the regressions (Bevis and Boutiouta) have a more pronounced daily cycle than the T_{m} calculated by ERA-Interim, because the T_{s} varies with a larger amplitude during a day than a mean (integrated) temperature.

A second important remark is that, for all stations, the mean bias between the Bevis-T_{m} and Boutiouta-T_{m} varies between 13.30 and 18 K. From Eqs. (12) and (13), it is already expected that, for the warmer temperatures of Algeria,

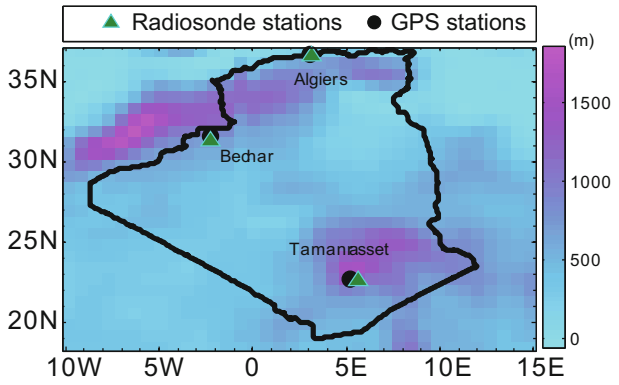

Fig. 1. Location of the GPS and radiosondes stations in Algeria used in the present study, with the surface height gridlines of ERA-Interim over-plotted.

the Bevis relationship will produce cooler mean temperatures than the Boutiouta regression. On the other hand, the mean bias between Bevis-T_{m} and ERA-Interim varies between −4 and 2 K only.

The regression of Boutiouta, which is formulated for Algeria, shows worse agreement with the ERA-Interim T_{m} than the regression of Bevis, which is based on radiosondes launched in the United States. To investigate the reason why the Boutiouta regression deviates so much from the other T_{m} formulations, we calculate the T_{m} directly from the radiosonde data in Algeria at these stations as the reference. The comparison is plotted in Fig. 3.

From Fig. 3, it can be seen that, for all stations, both during daytime and nighttime, a large bias between the T_{m} of Boutiouta and the other T_{m} formulations, and in particular with the T_{m} calculated from radiosondes, exists. The best agreement with the T_{m} calculated from the radiosondes is with the T_{m} of ERA-Interim, but at the Algiers station (0000 UTC), there are two outliers in the T_{m} calculated from the radiosonde data, which may point to some bad data. The good agreement between the T_{m} from the radiosondes and the T_{m} from ERA-Interim might be attributable to the impact that the assimilated radiosonde data has on the reanalysis. It can also be noted from Fig. 3 that the biases between the daytime and nighttime T_{m} values are larger for the T_{m} resulting from T_{m}–T_{s} regression (i.e., both Bevis and Boutiouta) than for the T_{m} calculated from ERA-Interim or from radiosondes. This feature is also clear in Fig. 2.

The distinct behavior of the Boutiouta T_{m}, especially with respect to the Bevis relationship, which is derived from radiosonde launches over the United States, might also be explained by the highly variable geography and climate of Algeria—a country of the subtropical zone where the dominant climate is hot and dry. Therefore, it might be very difficult to find one T_{m}–T_{s} relationship that could be applied to the whole the country. In this context, based on a study in Argentina, Fernández et al. (2010) concluded that the usage of T_{m} estimated from the Bevis model is the best choice for regional studies, unless further studies that take into account the geographical and climatological characteristics of the re-

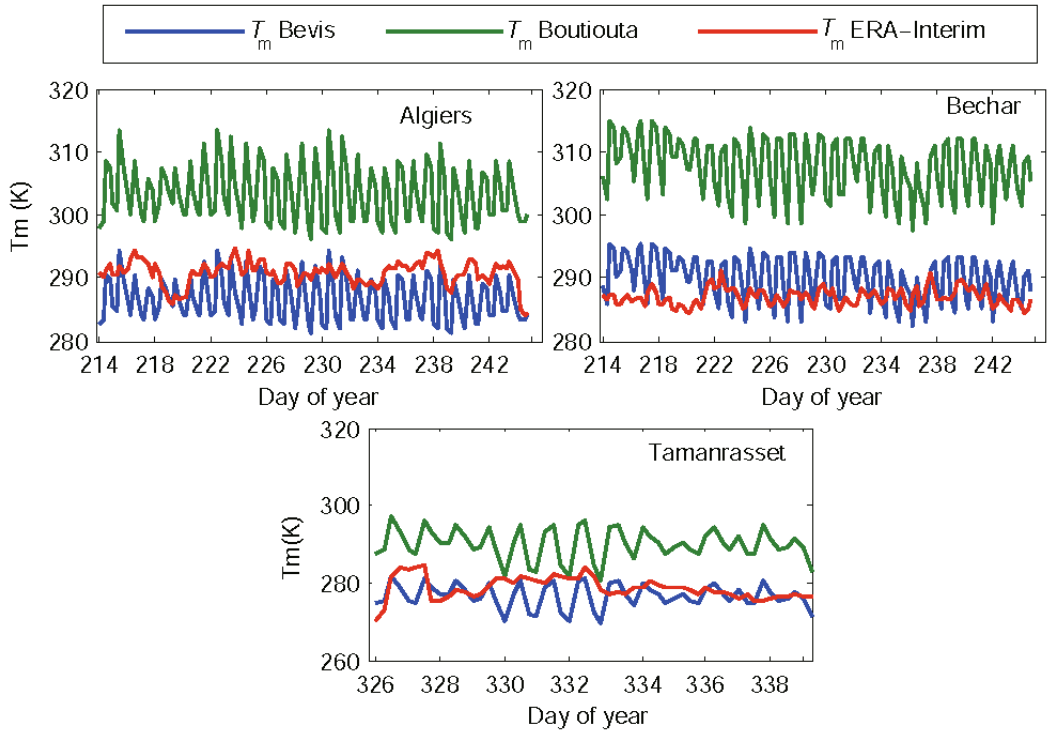

Fig. 2. Time series of different T_m estimations for the three Algerian stations of Algiers, Bechar (both for August 2012) and Tamanrasset (21 November to 4 December 2012).

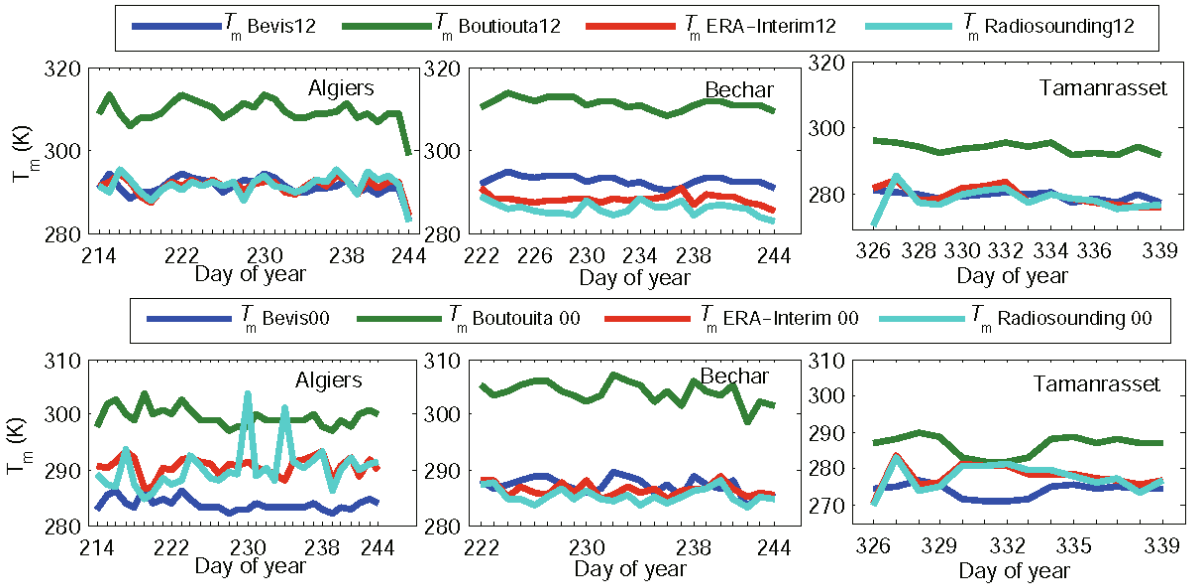

Fig. 3. Comparison of different T_m parameterizations during daytime (1200 UTC) and nighttime (0000 UTC).

gion are carried out. Such studies would provide a more suitable T_m model that is better adapted to the area. For Algeria, it seems that the parameterization of Boutiouta and Lahcene (2013) does not bring any added value related to geographical or climatological characteristics, as compared to the Bevis T_m parameterization. Looking at the linear T_m–T_s regression derived in Boutiouta and Lahcene (2013), their Fig. 2 shows a large standard deviation of 5 K. This value is comparable to the standard deviation obtained by Bevis et al. (1992) for their regression and radiosonde dataset, which encompasses a larger area and longer set of observations. Based on the Algerian radiosonde observations at the stations of Algiers and Tamanrasset for the year 2012, we also derive an alternative linear regression between T_m and T_s, $T_m = 0.45T + 148.30$,

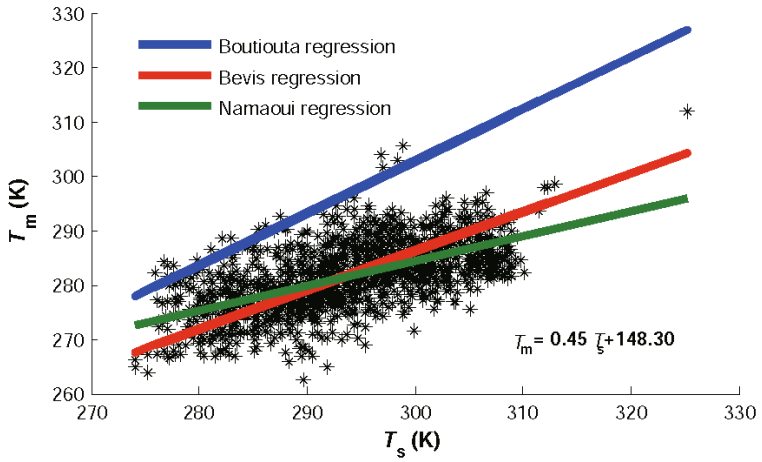

Fig. 4. Illustration of different $T_s - T_m$ regressions for the entire year in 2012 based on the radiosonde observations at Algiers and Tamanrasset stations.

with an RMSE equal to 4.82. (Fig. 4). Given there is an issue with the radiosonde T_s observations at Bechar for a large number of months in 2012, we cannot include this station in our linear regression. It is clear from Fig 4 that our regression is closer to the Bevis regression than to the Boutiouta and Lahcene (2013) regression. However, as our regression is only based on one year (2012) of radiosonde observations at two stations, we decide not to use this regression in the remainder of this paper.

6. Comparison of GPS-PW from different models of T_m

In this section we estimate and compare the GPS-PW from the T_m models based on the Bevis and Boutiouta regressions and ERA-Interim, which we refer to as Bevis-T_m PW, Boutiouta-T_m PW and ERA-T_m PW, respectively.

The different time series are presented in Fig. 5, from which we can see that the values of water vapor vary with the location of the station: a large difference in the PW range is observed between Algiers and Bechar for the same set of days. The maximum value of 51 mm is reached in August at Algiers, which is close to the sea, and the minimum value (of the order of 3.7 mm) is observed at Tamanrasset in November, because of the higher altitude and geographical location of this station (and the fact that for this station only winter measurements are available). For Bechar, the mean values of water vapor are in the order of 18 mm, i.e., between the Algiers and Tamanrasset ranges.

To illustrate the behaviour of GPS-PW with respect to the different T_m models, a comparative study is realized using different PW processing obtained with Boutiouta-T_m, Bevis-T_m and ERA-T_m. Since the Bevis model is a well-known standard reference, the Boutiouta-T_m and ERA-T_m GPS-PW differences are computed relative to this model reference and plotted in Fig. 6.

The largest difference between the Bevis- and Boutiouta-T_m GPS-PW recorded at Algiers is 2.59 mm. Whereas, for Bechar and Tamanrasset, the maximal differences are 1.63 and 1.22 mm, respectively.

The Bevis- and Boutiouta-T_m GPS-PW differences are negative for the three stations, meaning that the Boutiouta-T_m PW is higher than that of Bevis for all stations. This follows immediately from the distinctly higher T_m values obtained with the Boutiouta regression. The situation is quite different when applying ERA-T_m. In this case, for all stations the maximum PW difference with the Bevis-T_m GPS-PW does not exceed 1 mm, and the differences are sometimes positive and sometimes negative for the three stations. So, the better agreement of the T_m between the ERA-Interim calculation and the Bevis regression also results in smaller biases between the PW amounts, as compared to the Boutiouta-T_m regression.

It might seem remarkable that such a large bias in the T_m results in only a small bias in the GPS-PW. Therefore, to investigate the impact of T_m on the GPS-PW, we also use a statistical approach based on an error propagation law. According to Sapucci (2014), the effect of the uncertainties in T_m values σ_{T_m} on GPS-PW estimations is given by the following equation:

$$\sigma_{pw}^2 = \left[10^6 \mathrm{ZWD} R_w \frac{k_3}{(R_w k_3 + R_w k_2' T_m)^2}\right] \sigma_{T_m}^2 . \qquad (15)$$

By setting the values of T_m uncertainties σ_{T_m} in the range of 10 to 1 K according to the results illustrated in Fig. 2, the obtained values of σ_{pw} indicate that the impact of T_m on GPS-PW varies from station to station: for Algiers, the effect of the T_m bias on GPS-PW is of the order of 2.01 mm. On the other hand, the impact of the T_m bias on GPS-PW varies by around 1.57 and 1.19 mm at Bechar and Tamanrasset, respectively. These calculations show that the uncertainty of the T_m values produces small differences in the final estimation of GPS-PW, which do not exceed 2 mm. Fernández et al. (2010) also found differences between different parameterizations of T_m, of the order of 15 K, in Argentina, but this only produces small differences in the final evaluation of PW. For instance,

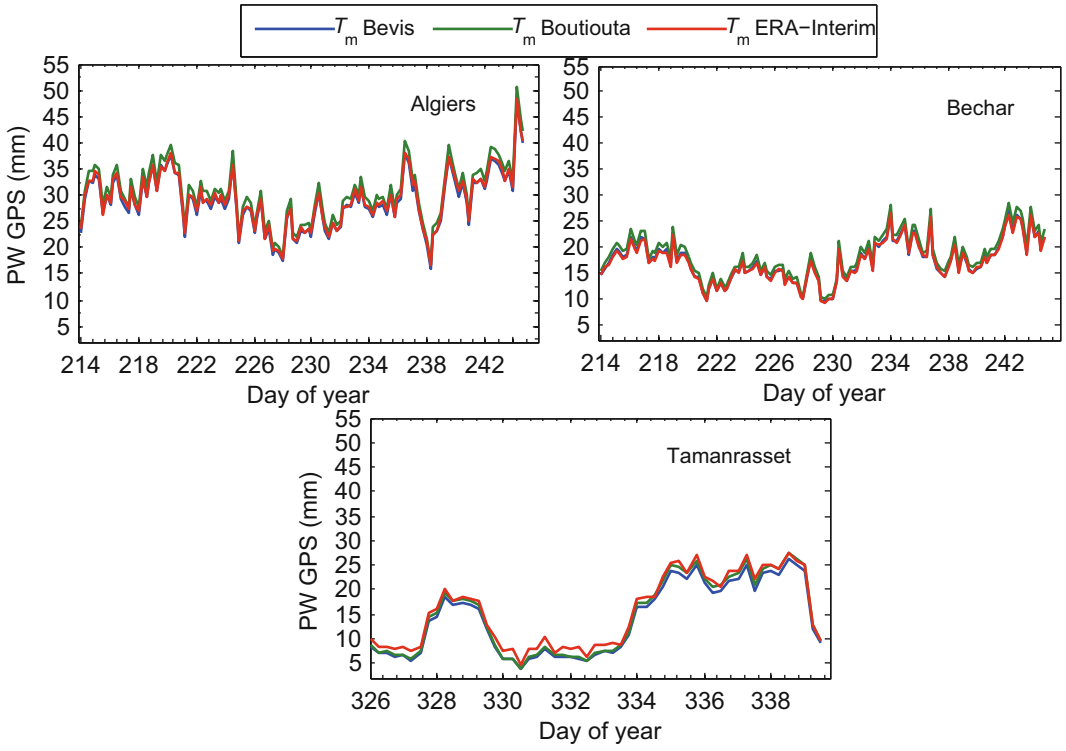

Fig. 5. Time series of PW from different T_m parameterizations for Algiers, Bechar (both for August 2012) and Tamanrasset (21 November to 4 December 2012).

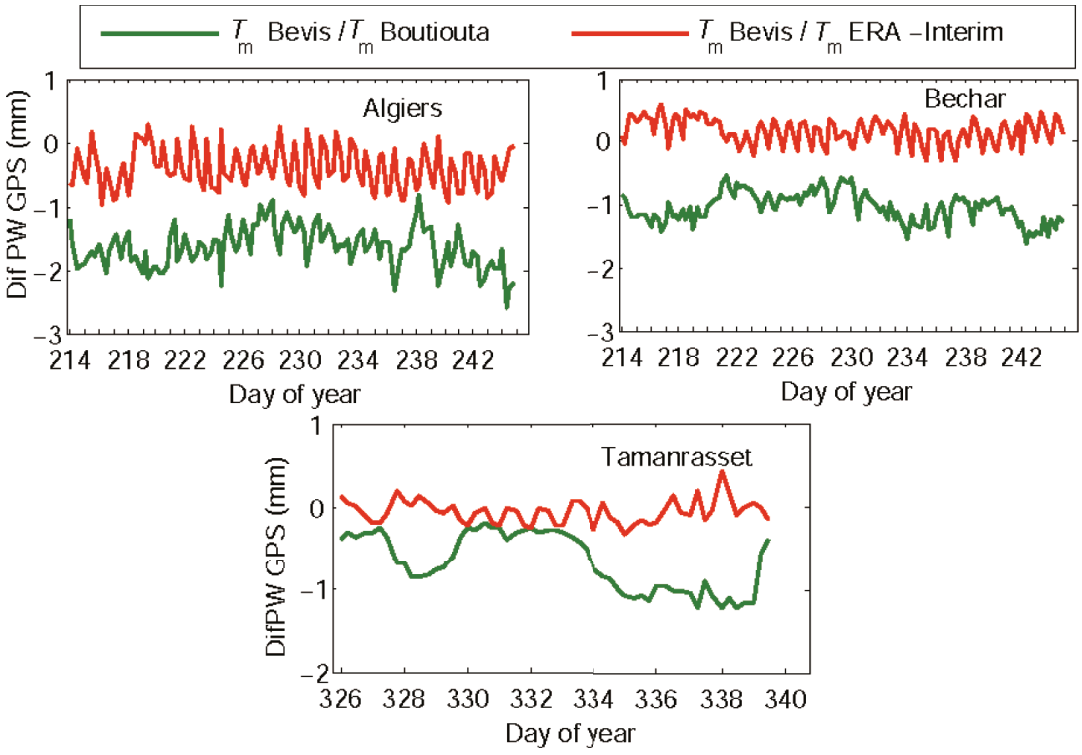

Fig. 6. Differences of precipitable water (DifPW) from different T_m parameterizations at Algiers, Bechar and Tamanrasset.

the differences between the GPS-PW estimated with Bevis-T_m, with respect to T_m ERA reanalysis, can be as large as 3 mm during wet or very rainy periods. Van Malderen et al. (2014) mentioned that the uncertainty of T_m is estimated to be around 5 K (or 1.8 % for $T_m = 273$ K), which corresponds to a PW error of 0.07 to 0.72 mm for a dry or moist atmosphere, respectively.

7. Validation of GPS-PW with radiosondes and ERA-Interim

7.1. *Radiosondes*

In this section we compare the GPS-PW retrievals with the PW calculated from the integration of the vertical profiles measured with radio soundings (RS-PW).

The scatter plots of all observations (at both 0000 and 1200 UTC) of GPS-PW against RS-PW can be seen in Fig. 7, together with the fitted linear regressions. The statistical parameters of the scatter plots and the differences are summarized in Table 3, again at both 0000 and 1200 UTC. These are: the average of the differences [mean bias error (MBE)] and the root-mean-square error (RMSE) of the differences calculated between RS-PW and the GPS-PW of the three T_m models, i.e., ERA-T_m minus RS-PW, Bevis-T_m minus RS-PW, and Boutiouta-T_m minus RS-PW (units: mm). The correlation coefficient (R^2) between RS-PW and GPS-PW, computed from the different T_m parameterizations, is also given.

A fairly good agreement can be observed between the RS-PW and GPS-PW over all stations, except for Algiers, where

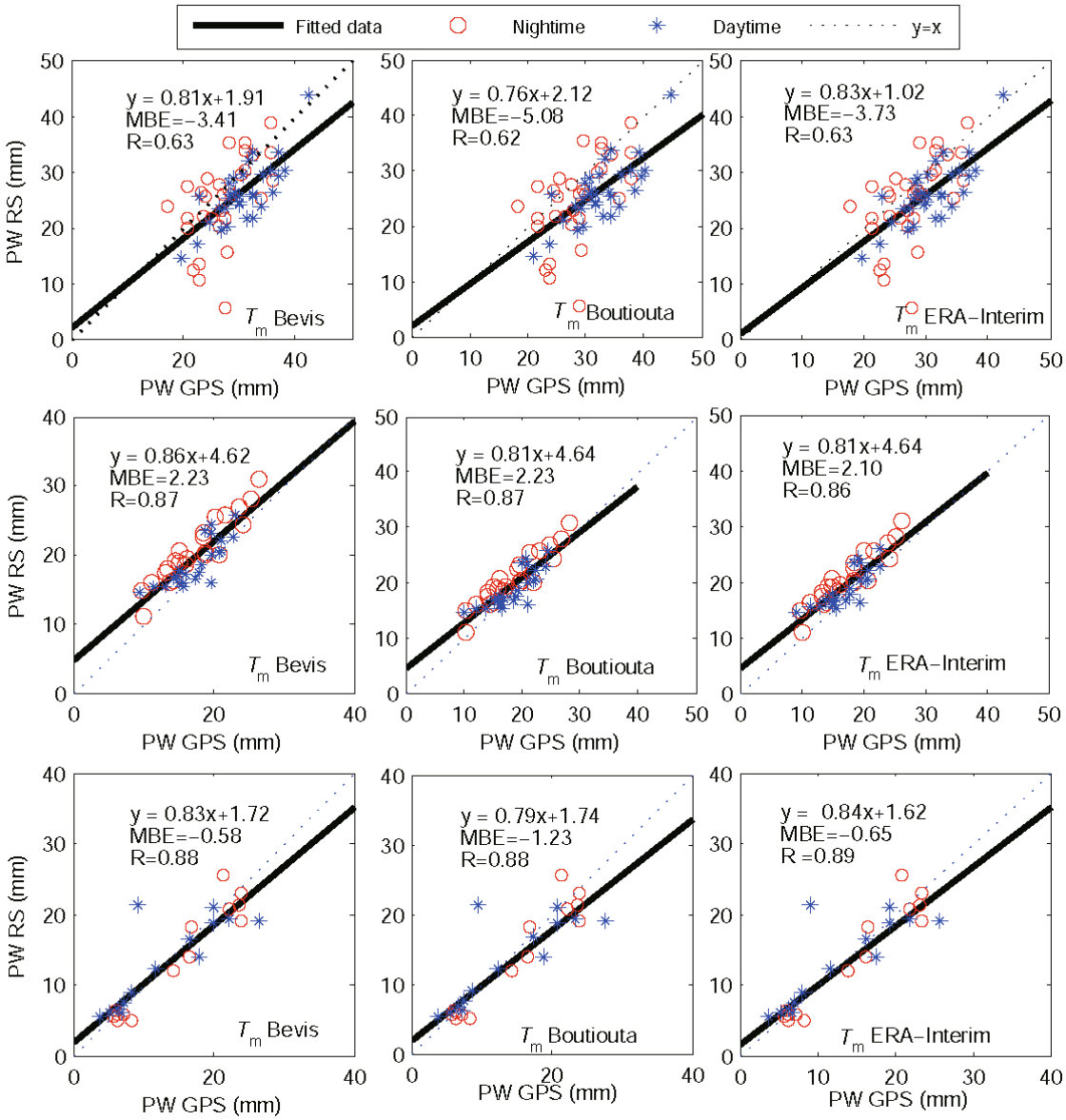

Fig. 7. Scatter plots of all observations of GPS-PW and RS-PW at Algiers (upper panels), Bechar (middle panels), and Tamanrasset (lower panels).

Table 3. Statistical comparison between GPS-PW and RS-PW. The MBE is the mean PW difference taken as GPS minus RS.

Station	T_m	1200 UTC			0000 UTC		
		RMSE	MBE	R^2	RMSE	MBE	R^2
Algiers	ERA-Interim	3.24	−4.49	0.77	3.91	2.09	0.62
	Bevis	3.16	−4.5	0.77	3.84	1.48	0.63
	Boutiouta	3.34	−5.40	0.77	4.07	−2.95	0.3
Bechar	ERA-Interim	1.54	−2.27	0.89	1.35	−0.89	0.95
	Bevis	1.90	0.94	0.88	1.95	−2.92	0.92
	Boutiouta	1.92	−0.53	0.86	2.06	1.89	0.92
Tamanrasset	ERA-Interim	0.92	−0.68	0.99	2.90	−0.29	0.92
	Bevis	0.98	−0.74	0.99	2.92	−0.15	0.92
	Boutiouta	1.03	−1.43	0.99	3.06	−0.76	0.92

the correlation coefficient is only around 0.60. This station has a strong outlier with an overly low PW value of around 5 mm measured by the radiosonde. But, in general, this station also has the largest RMSE (in the range of 3–4 mm) of the three sites. This GPS station is also characterized by a large daytime dry bias of around 5 mm, compared to the RS observations. On the other hand, the GPS station has a wet nighttime bias of around 2 mm for Bevis- and ERA-T_m estimations. The origin of these large mean differences might be related to the GPS-PW retrieval (for example, multipath near the GPS antenna), or to the inferior quality of the radiosonde type (MODEM M2K2-DC) used at this station. During the last World Meteorological Organization (WMO) radiosonde intercomparison campaign (Nash et al., 2011), the systematic bias estimates showed that MODEM nighttime relative humidity measurements had large positive bias greater than 10% for much of the time in the lower and middle troposphere, which were presumed to be due to the application of solar dry bias correction at night. Biases of this magnitude were also seen in the 2005 Mauritius test. The MODEM daytime relative humidity measurements did not show these positive biases. This was also reflected in the MODEM RS-PW having a more pronounced positive bias (of almost 10 mm) in the nighttime observations compared to daytime, with respect to the GPS-PW measurements at the intercomparison site (Nash et al., 2011, Fig. 8.4.2). Comparisons of M2K2DC measurements to GPS-PW performed at Nîmes and Ajaccio, France, also showed a moist bias at night, typically of 5% to 10 % (Bock et al., 2013). Although the sign of the daytime and nighttime GPS–RS differences found in our study is opposite to those reported in this intercomparison campaign, it points to some issues with the MODEM radiosondes. As a matter of fact, during a campaign at Observatoire Haute Provence, France, in 2011, the MODEM M2K2DC had a dry bias of −5% RH up to 6 km, which decreased above compared to other radiosonde measurements, and consistently showed large dry biases with the GPS-PW measurements at the site, also at night (Bock et al., 2013).

For Bechar and Tamanrasset stations, the correlation coefficients are higher (around 0.88 for all observations, but even between 0.92 and 0.99 if we separate the daytime and nighttime observations), the RMSE ranges between 1 to 3 mm, and GPS-PW biases are mostly dry and below 2 mm. For Bechar, the biases vary significantly among the different T_m parameterizations, and between daytime and nighttime. The lower biases of these stations compared to the Algiers site might also be related with the differences in expected offsets due to the height differences between the GPS and RS launch sites. We estimate an offset of the order of 0.38 mm for Algiers (more humid atmosphere), but one not exceeding 0.2 mm for the other two stations, located in a drier environment. Indeed, we observe that as it gets drier here, the bias does reduce. It should, however, be noted that the observed biases here are larger than we derived from their height differences.

Comparing the daytime and nighttime measurements, we can conclude that, for Algiers and Tamanrasset, the daytime observations show a better agreement (lower RMSE, higher correlation coefficients), but with larger dry biases than the nighttime measurements. These conclusions for Algiers and Tamanrasset are valid for the three different parameterizations. For Bechar, the different parameterizations affect the comparison of the daytime and nighttime measurements differently, except for the correlation coefficients: these are higher for the nighttime measurements.

The slopes of the linear regression lines of the scatter plots in Fig. 7 are, for all three stations, below 1, which means that, with intercepts larger than 1, for larger PW ranges, the GPS retrieval gives higher PW values than the co-located RS observations, while the opposite is true for the lower PW values. As a consequence, if we ignore the instrumental biases (intercepts), the GPS technique seems more sensitive for measuring high-end PW ranges, while the RS approach seems more sensitive for measuring low-end PW ranges. This has also been noted by Van Malderen et al. (2014) for a worldwide GPS–RS PW intercomparison, performed at nearly 30 sites.

We find that the total uncertainty of GPS-based PW measurements in Algeria is generally less than 2 mm if compared with radiosonde PW observations, except at the Algiers station, which is equipped with MODEM M2K2-DC radiosondes. This estimation agrees with previous studies where GPS-PW uncertainties were obtained by comparison with radiosondes (Businger et al., 1996; Duan et al., 1996; Teregoning et al., 1998, and other references in Van Malderen et al., 2014). We also eliminate some outliers that affect our statistical study and, consequently, a significant improvement is found in the parameters (MBE and R^2). For example, for the Algiers station, the MBE decreases from −5.08 to −3.90 mm and the R^2 increases from 0.62 to 0.71.

7.2. *ERA-Interim*

As in the comparison between GPS-PW and RS-PW, the scatter plots and statistical parameters of the comparison between GPS-PW ERA-Interim are shown in Fig. 8 and Table 4, respectively.

The results are comparable with the GPS-PW–RS-PW comparison, in the sense that the correlation coefficients and the RMSE are hardly affected by which parameterization

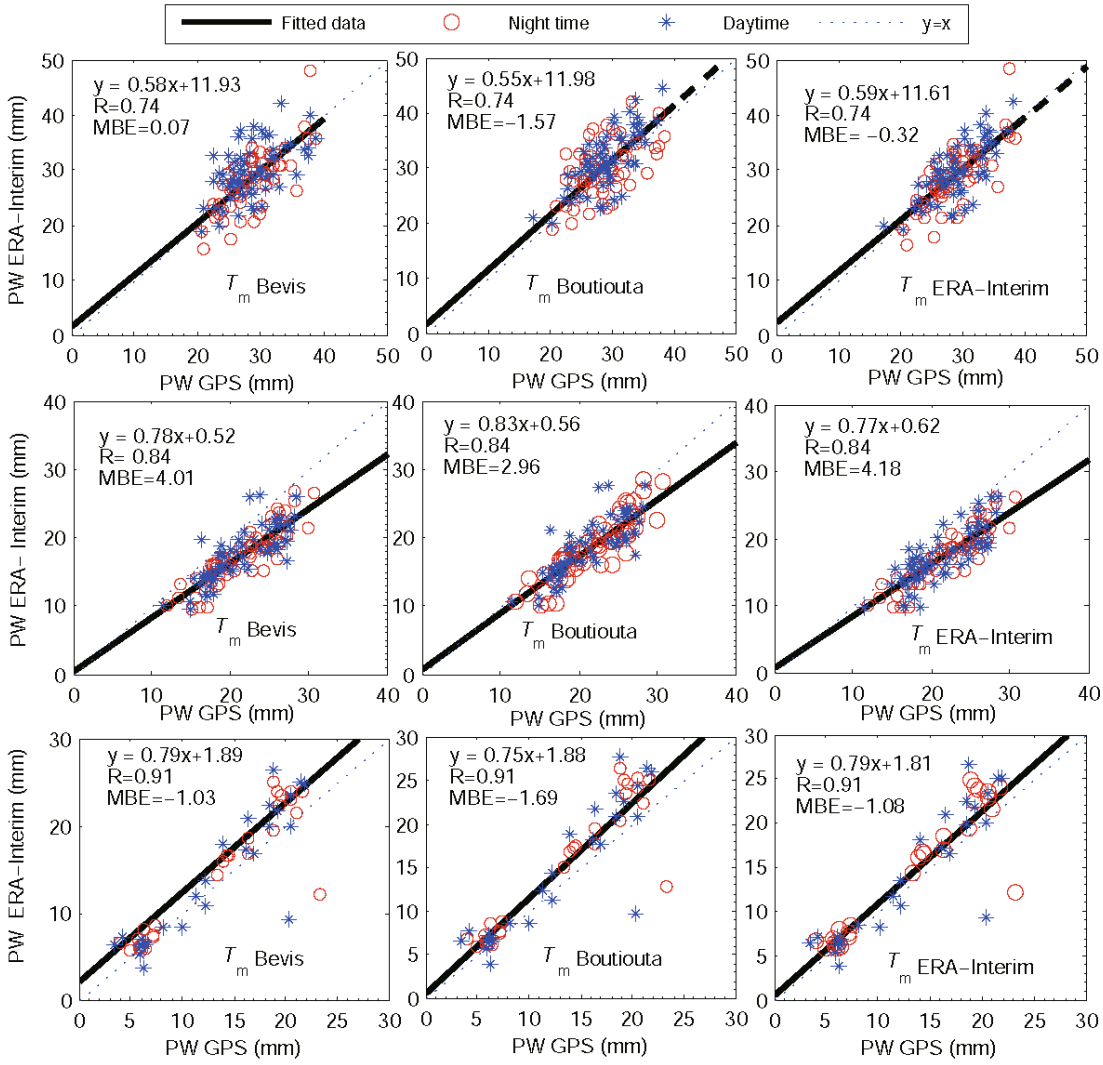

Fig. 8. Scatter plots of all observations of GPS-PW and the PW of ERA-Interim at Algiers (upper panels), Bechar (middle panels), and Tamanrasset (lower panels).

Table 4. Statistical comparison between GPS-PW and the PW of ERA-Interim. The MBE is the mean PW difference taken as GPS minus RS.

		1200 UTC			0000 UTC		
Station	T_m	RMSE	MBE	R^2	RMSE	MBE	R^2
Algiers	ERA-Interim	2.87	−1.75	0.75	3.08	1.12	0.72
	Bevis	2.879	−1.77	0.75	3.12	1.73	0.72
	Boutiouta	2.88	−3.63	0.75	3.12	0.26	0.72
Bechar	ERA-Interim	2.34	4.23	0.81	1.98	4.03	0.92
	Bevis	2.33	3.85	0.81	1.94	3.94	0.91
	Boutiouta	2.33	3.85	0.81	1.94	3.94	0.92
Tamanrasset	ERA-Interim	1.39	−1.03	0.97	2.01	−0.59	0.95
	Bevis	1.44	−1.09	0.97	2.04	−0.42	0.95
	Boutiouta	1.44	−1.77	0.97	2.05	−1.03	0.95

is used for T_m, while the differences are more noticeable in the regression slopes and biases. Also, for the comparison of daytime and nighttime measurements, the daytime observations at Algiers and Tamanrasset show a better agreement (lower RMSE, higher correlation coefficients), but with larger dry biases than the nighttime measurements. For Bechar, there is a better agreement for the nighttime observations (lower RMSE, higher correlation coefficients), with comparable biases for the daytime and nighttime observations. The linear regression slopes are lower than 1 for all sites, but closer to 1 for the stations with the lowest PW range.

For the Algiers station, the GPS-PW compares better with that of ERA-Interim for all statistical parameters and at both time-stamps, whereas exactly the opposite is true at Bechar. This can probably be explained by the model sensitivity to topography. Bechar is surrounded by a mountain range that has three summits on the top of the Saoura valley at altitudes varying between 1200 and 1900 m, so that the PW contributions of the four grid points surrounding this station in the ERA-Interim grid might differ significantly (see Fig. 1). This result is in agreement with a previous study (Mengistu Tsidu et al., 2015). For Tamanrasset, the GPS-PW agrees

best with RS-PW for the daytime observations; whereas, for the nighttime measurements, the agreement is better with the PW of ERA-Interim, except for the biases. This station also has a distinct geography, being surrounded by several streambeds (these remaining dry except during the rainy season), so called Oueds (in our case the Oueds of Tamanrasset, Sersouf and Tahaggart).

We also test the impact of outliers on our comparison. For example, after removal of the outliers at Bechar, the MBE decreases from 4.01 to 2.9 and the R^2 increases from 0.84 to 0.90.

8. Conclusion

This study gives some first results on comparing different PW data sources for three stations in Algeria (Algiers, Bechar and Tamanrasset). In particular, we analyze the impact of the weighted mean temperature T_m on the retrieved GPS–PW by comparing three different T_m parameterizations [the T_m–T_s linear regression of Bevis et al. (1992), the T_m–T_s linear regression for Algeria from Boutiouta and Lahcene (2013), and the T_m calculated from ERA-Interim]. The results indicate that the differences in T_m are of the order of 18 K, producing differences of 2.01 mm in the final evaluation of PW.

A good agreement between GPS and radiosondes is found, with mean differences less than 2 mm, except at the Algiers station, which is the only station of our sample with MODEM M2K2-DC radiosonde launches.

The comparison between the PW of ERA-Interim and GPS-PW shows differences in the magnitude and sign of the bias that vary from station to station. Algeria is a country that has a very large area and, consequently, the northern part has a Mediterranean climate, while the rest of the country mostly has a desert climate. However, between these two major climate types, transitional climate zones exist, including the semi-arid type. Therefore, the choice of T_m must be established according to different climatic regions.

We find that the T_m of ERA-Interim is closest to the reference (T_m calculated directly from the radiosondes). In this context, we suggest using the T_m of ERA-Interim for all applications of GNSS and meteorology in Algeria, given the lack of radiosonde stations in the north of Algeria, and the weak correlation between T_s and mean temperature in large-area countries like Algeria, as illustrated by the poor performance of the T_m–T_s linear regression of Boutiouta in comparison with the other T_m estimations.

In summary, the intercomparison of different instruments and reanalysis over Algeria is the first step for any application of GNSS and meteorology. This study will serve as a starting point from which further studies will be conducted for the validation of satellite products (e.g., for AIRS and MODIS), to improve our understanding of the water vapor mechanism.

Acknowledgements. The authors would like to thank the National Institute of Cartography and Remote Sensing and the Algerian Research Center for Astronomy, Astrophysics and Geophysics, for providing the GPS data. We are also grateful to Mr Larry OOLMAN from the University of Wyoming for making available the archive data of weather stations in Algeria.

REFERENCES

Askne, J., and H. Nordius, 1987: Estimation of tropospheric delay for microwaves from surface weather data. *Radio Sci*., **22**, 379–386, doi: 10.1029/RS022i003p00379.

Bevis, M., S. Businger, T. A. Herring, C. Rocken, R. A. Anthes, and R. H. Ware, 1992: GPS meteorology: Remote sensing of atmospheric water vapor using the global positioning system. *J. Geophys. Res*., **97**, 15 787–15 801, doi: 10.1029/92 JD01517.

Bevis, M., S. Businger, S. Chiswell, T. A. Herring, R. A. Anthes, C. Rocken, and R. H. Ware, 1994: GPS Meteorology: Mapping zenith wet delays onto precipitable water. *J. Appl. Meteor*., **33**, 379–386.

Bock, O., and Coauthors, 2013: Accuracy assessment of water vapour measurements from in situ and remote sensing techniques during the DEMEVAP 2011 campaign at OHP. *Atmospheric Measurement Techniques*, **6**, 2777–2802, doi: 10.5194/amt-6-2777-2013.

Boutiouta, S., and A. Lahcene, 2013: Preliminary study of GNSS meteorology techniques in Algeria. *Int. J. Remote Sens*., **34**, 5105–5118.

Brenot, H., V. Ducrocq, A. Walpersdorf, C. Champollion, and O. Caumont, 2006: GPS zenith delay sensitivity evaluated from high-resolution numerical weather prediction simulations of the 8-9 September 2002 flash flood over southeastern France. *J. Geophys. Res*., **111**, doi: 10.1029/2004JD005726.

Businger, S., Chiswell, S. R., Ulmer, W. C., and Johnson, R., 1996: Balloons as a Lagrangian measurement platform for atmospheric research. *J. Geophys. Res*, **101**, doi: 10.1029/95JD 00559.

Davis, J. L., T. A. Herring, I. I. Shapiro, A. E. E. Rogers, and G. Elgered, 1985: Geodesy by radio interferometry: Effects of atmospheric modeling errors on estimates of baseline length. *Radio Sci*., **20**, 1593–1607, doi: 10.1029/RS020i006p01593.

Dee, D. P., and Coauthors 2011: The ERA-Interim reanalysis: Configuration and performance of the data assimilation system. *Quart. J. Roy. Meteorol. Soc*., **137**, 553–597. doi: 10.1002/ qj.828.

Duan J., and Coauthors, 1996: GPS meteorology: Direct estimation of the absolute value of precipitable water. *J. Appl. Meteorol.*, **35**, 830–838.

Elliott, W. P., 1995: On detecting long-term changes in atmospheric moisture. *Climatic Change*, **31**, 349–367, doi: 10.1007/BF01095152.

Fernández, L. I., P. Salio, M. P. Natali, and A. M. Meza, 2010: Estimation of precipitable water vapour from GPS measurements in Argentina: Validation and qualitative analysis of results. *Advances in Space Research*, **46**, 879–894, doi: 10.1016/j.asr. 2010.05.012.

Guerova, G., E. Brockmann, J. Quiby, F. Schubiger, and C. Matzler, 2003: Validation of NWP mesoscale models with Swiss GPS network AGNES. *J. Appl. Meteor*., **42**, 141–150.

Guerova, G., and Coauthors, 2016: Review of the state of the art and future prospects of the ground-based GNSS meteorology in Europe. *Atmospheric Measurement Techniques*, **9**, 5385–

5406.

Kos, T., M. Botinčan, and A. Dlesk, 2009: Mitigating GNSS Positioning Errors due to Atmospheric Signal Delays. *Pomorstvo*, **23**, 495–513.

Mengistu Tsidu, G., T. Blumenstock, and F. Hase, 2015: Observations of precipitable water vapour over complex topography of Ethiopia from ground-based GPS, FTIR, radiosonde and ERA-Interim reanalysis. *Atmospheric Measurement Techniques*, **8**, 3277–3295, doi: 10.5194/amt-8-3277-2015.

Nash, J., T. Oakley, H. Vömel, and L. I. Wei, 2011: WMO intercomparison of high quality radiosonde systems, Yangjiang, China, 12 July–3 August 2010. IOM Rep. 107, WMO/TD 1580, World Meteorological Organization, 238 pp.

Niell, A. E., 1996: Global mapping functions for the atmosphere delay at radio wavelengths. *J. Geophys. Res.*, **101**, 3227–3246.

Rocken, C., T. Van Hove, and R. Ware, 1997: Near real-time GPS sensing of atmospheric water vapor. *Geophys. Res. Lett.*, **24**, 3221–3224.

Saastamoinen, J., 1972: Atmospheric correction for the troposphere and stratosphere in radio ranging of satellites. *The Use of Artificial Satellites for Geodesy*, S. W. Henriksen, A. Mancini, and B. H. Chovitz, AGU, Washington, D.C., 247–251.

Sapucci, L. F., 2014: Evaluation of modeling water-vapor-weighted mean tropospheric temperature for GNSS-integrated water vapor estimates in Brazil. *Journal of Applied Meteorology and Climatology*, **53**, 715–730, doi: 10.1175/JAMC-D-13-048.1.

Teregoning, P., Boers, R. O'Brier, D., Hendy, M., 1998: Accuracy of absolute precipitable water vapor estimates from GPS observations. *J. Geophys. Res.*: Atmopsheres, 103, 28.

Thayer, G. D., 1974: An improved equation for the radio refractive index of air. *Radio Sci.*, **9**, 803–807.

Torres, B., V. E. Cachorro, C. Toledano, J. P. Ortiz de Galisteo, A. Berjón, A. M. de Frutos, Y. Bennouna, and N. Laulainen, 2010: Precipitable water vapor characterization in the Gulf of Cadiz region (southwestern Spain) based on Sun photometer, GPS, and radiosonde data. *J. Geophys. Res.*, **115**, doi: 10.1029/2009JD012724.

Van Malderen, R., and Coauthors, 2014: A multi-site intercomparison of integrated water vapour observations for climate change analysis. *Atmospheric Measurement Techniques*, **7**, 2487–2512, doi: 10.5194/amt-7-2487-2014.

Vey, S., R. Dietrich, M. Fritsche, A. Rülke, P. Steigenberger, and M. Rothacher, 2009: On the homogeneity and interpretation of precipitable water time series derived from global GPS observations. *J. Geophys. Res.*, **114**, doi: 10.1029/2008JD 010415.

Wang, J. H., and L. Y. Zhang, 2008: Systematic errors in global radiosonde precipitable water data from comparisons with ground-based GPS measurements. *J. Climate*, **21**, 2218–2238, doi: 10.1175/2007JCLI1944.1.

Ware, R. H., and Coauthors, 2000: Suominet: A real-time national GPS network for atmospheric research and education. *Bull. Amer. Meteor. Soc.*, **81**, 677–694.